Technical Notes

Convection Heat Transfer in Water at 4°C Past Vertical Slender Cylinders

C. Kleinstreuer* and Tian-Yih Wang†
North Carolina State University, Raleigh, North Carolina

Nomenclature

D = diameter of cylinder
f = dimensionless stream function
Gr = Grashof number based on r_0
Gr_L = Grashof number based on L
Gr_x = Grashof number based on x
g = gravitational acceleration
h = local heat-transfer coefficient
k = thermal conductivity
L = characteristic length
m_x = dimensionless parameter (Sec. 4B)
Nu_x = local Nusselt number
Pr = Prandtl number
q = heat flux
Ra = Rayleigh number based on r_0
Ra_L = Rayleigh number based on L
Ra_x = Rayleigh number based on x
Re = Reynolds number based on r_0
Re_L = Reynolds number based on L
Re_x = Reynolds number based on x
r = radial coordinate
r_0 = radius of cylinder
T = temperature
u = velocity components in x-direction
u_∞ = freestream or outer flow velocity
v = velocity components in r-direction
x = longitudinal coordinate
Z = index for operational mode ($Z = 1 \hat{=}$ heated cylinder, $Z = -1 \hat{=}$ cooled cylinder)
α = thermal diffusivity
β = coefficient of thermal expansion
γ = coefficient of thermal expansion of water at 4°C
η = similarity variable
ξ = dimensionless parameter
ν = kinematic viscosity
ρ = density
θ = dimensionless temperature
Λ = transverse-curvature parameter (free convection)
λ = transverse-curvature parameter (mixed convection)
ψ = stream function

I. Introduction

BUOYANCY-DRIVEN flows of water along vertical slender cylinders under the condition of a density extremum may arise in freezing or deicing processes, Earth-coupled heat pump systems, and vertical pipe networks in reservoirs. Free and mixed convection heat transfer on a vertical cylinder has been studied by Sparrow and Gregg,[1] Wilks,[2] Minkowycz and Sparrow,[3] and Bui and Cebeci,[4] among others. These analyses are confined to fluids in room temperature ranges. They are not applicable to convection heat transfer in water at 4°C ± 4°C where its density has a maximum at atmospheric pressure. In the neighborhood of this special point, density variations can be expressed[5] as $\Delta\rho = -\rho_0\gamma(\Delta T)^2$, whereas a linear variation is sufficient at other reference temperatures with small deviations, i.e., $\Delta\rho = -\rho_0\beta\Delta T$, where $\beta = \beta(T_{ref})$.

Several authors[5-7] used water at 4°C as a fluid and, hence, the nonlinear Boussinesq approximation for $\Delta\rho$ to analyze free forced convection heat transfer, usually along a vertical, semi-infinite flat plate. A most recent exception is the paper by Gorla and Stratman[7] who considered natural convection past a slender cone.

Of interest here is a comprehensive, computationally efficient analysis of steady laminar axisymmetric flow with free or mixed thermal convection in water at about 4°C past a vertical cylinder with transverse curvature effects. The cylinder can be either heated ($T_w > T_\infty$) or cooled ($T_w < T_\infty$). The coupled nonlinear boundary-layer equations are transformed using new combined variables based on scale analysis for easier numerical simulation. Numerical criteria are given for cases when curvature effects are negligible and equivalent, flat-plate Nusselt number correlations can be used.

II. Analysis

Consider steady laminar axisymmetric boundary-layer flow of a maximum density fluid past a vertical slender cylinder at uniform temperature (Fig. 1). Using the nonlinear Boussinesq

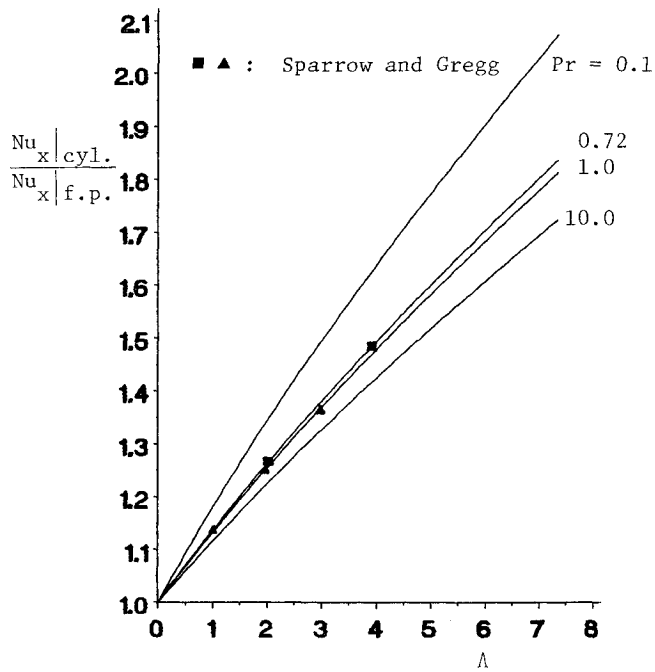

Fig. 1 Ratio of local Nusselt numbers of vertical slender cylinder and flat plate for various Prandtl numbers: free convection case, linear $\rho(\Delta T)$.

Received June 29, 1987; revision received Oct. 23, 1987.

*Associate Professor, Mechanical and Aerospace Engineering Department.
†Graduate Research Assistant, Mechanical and Aerospace Engineering Department.

approximation discussed in the previous section, the governing equations are:[8]

$$\frac{\partial(ru)}{\partial x} + \frac{\partial(rv)}{\partial r} = 0 \tag{1}$$

$$u\frac{\partial u}{\partial x} + v\frac{\partial v}{\partial x} = Zg\gamma(T - T_\infty)^n + \frac{\nu}{r}\frac{\partial}{\partial r}\left(r\frac{\partial u}{\partial r}\right) \tag{2}$$

$$u\frac{\partial T}{\partial x} + v\frac{\partial T}{\partial r} = \frac{\alpha}{r}\frac{\partial}{\partial r}\left(r\frac{\partial T}{\partial r}\right) \tag{3}$$

where the exponent $n = 2$ for water at approximately 4°C. Elsewhere, $n = 1$ and $\gamma \equiv \beta$. The associated boundary conditions for the cases of natural and mixed thermal convection are:

$$u = v = 0 \quad \text{and} \quad T = T_w \quad \text{at} \quad r = r_0 \tag{4a}$$

and for natural convection

$$u = v = 0 \quad \text{and} \quad T = T_\infty \quad \text{when} \quad r \to \infty \tag{4b}$$

and for mixed convection

$$u = u_\infty, \quad v = 0 \quad \text{and} \quad T = T_\infty \quad \text{when} \quad r \to \infty \tag{4c}$$

A. Natural Convection Case

The following combined variables based on scale analysis are introduced[9]:

$$\xi = x/r_0 \tag{5a}$$

$$\eta = [(r^2 - r_0^2)/8xr_0]Ra_x^{1/4} \tag{5b}$$

$$\psi = \alpha r_0 Ra_x^{1/4} f(\eta) \tag{5c}$$

$$\theta(\eta) = (T - T_\infty)/(T_w - T_\infty) \tag{5d}$$

where

$$Ra_x = (g\gamma/\nu\alpha)(T_w - T_\infty)^2 x^3 \tag{5e}$$

Since the stream function approach satisfies the continuity equation automatically, the transformed governing equations read

$$(1/Pr)(2f'^2 - 3ff'') = [(1 + \Lambda\eta)f'']' + 64 - \theta^2 \tag{6}$$

and

$$[(1 + \Lambda\eta)\theta']' + 3f\theta' = 0 \tag{7}$$

subject to

$$f = f' = 0 \quad \text{and} \quad \theta = 1 \quad \text{for} \quad \eta = 0 \tag{8a}$$

and

$$f' = 0 \quad \text{and} \quad \theta = 0 \quad \text{for} \quad \eta \to \infty \tag{8b}$$

The parameter Λ reflects transverse curvature and is defined as

$$\Lambda = 8(\xi/Ra)^{1/4} \tag{8c}$$

where

$$Ra = \frac{g}{\alpha}\frac{\gamma}{\nu}(T_w - T_\infty)^2 r_0^3 \tag{8d}$$

Curvature effects are negligible for free convection on long cylinders, where $\Lambda \to 0$.

B. Combined Free-Forced Convection Case

For mixed thermal convection, a slightly different set of transformed variables are used, again based on scale analysis in order to reduce Eqs. (2) and (3) to

$$[(1 + \lambda\eta)f'']' + \tfrac{1}{2}ff'' = -Z\xi\theta^2 + \xi\left[f'\frac{\partial f'}{\partial \xi} - f''\frac{\partial f}{\partial \xi}\right] \tag{9}$$

$$(1/Pr)[(1 + \lambda)\eta\theta']' + \tfrac{1}{2}f\theta' = \xi\left[f'\frac{\partial \theta}{\partial \xi} - \theta'\frac{\partial f}{\partial \xi}\right] \tag{10}$$

The boundary conditions are

$$f = f' = 0 \quad \text{and} \quad \theta = 1 \quad \text{for} \quad \eta = 0 \tag{11a}$$

$$f' = 1, \quad \theta = 0 \quad \text{for} \quad \eta \to \infty \tag{11b}$$

The system variables of Eqs. (9) and (10) are defined as

$$\xi = (Gr_x/Re_x^2) \sim x \tag{12a}$$

$$Re_x = (u_\infty x/\nu) \tag{12b}$$

$$\eta = [(r^2 - r_0^2)/2xr_0]Re_x^{1/2} \tag{12c}$$

$$Gr_x = [g\gamma(T_w - T_\infty)^2 x^3/\nu^2] \tag{12d}$$

$$\psi = (u_\infty r_0 x/Re_x^{1/2})f(\xi,\eta) \tag{12e}$$

$$\theta(\xi,\eta) = [(T - T_\infty)/(T_w - T_\infty)] \tag{12f}$$

$$Z = \begin{cases} 1 & \text{for heated cylinder} \\ -1 & \text{for cooled cylinder} \end{cases} \tag{12g}$$

The transverse curvature parameter is defined as[4]

$$\lambda = 2[\xi/(Gr/Re)]^{1/2} \tag{12h}$$

with

$$Re = u_\infty r_0/\nu \tag{12i}$$

$$Gr = g\gamma(T_w - T_\infty)^2 r_0^3/\nu^2 \tag{12j}$$

III. Numerical Solution Method

The transformation of the governing equations reduced the x-dependence and, hence, the numerical work significantly. The free convection problem (cf. Sec. IIA) can be readily solved with a standard numerical scheme such as the Runge-Kutta algorithm. We employed Keller's Box method[10] for both cases using a nonuniform mesh in both directions, i.e., r and x. Special care was required for the mixed thermal convection case (cf. Sec. IIB) because of the singular point $\xi = 0$ where a very fine grid size was needed to compute the velocity and temperature profiles. For the case of high curvature, e.g., $\lambda = 0.63$, the largest nonuniform mesh consisted of 117 nodal points in the r-direction and 200 points in the x-direction. The independence of the results on the mesh density has been checked.

IV. Results and Discussion

The results of the computer simulation study are grouped into two categories representing free convection and mixed free-forced convection. With the verified computer code, transverse-curvature effects on the heat-transfer mechanisms have been analyzed, and numerical values have been determined for specific dimensionless groups that indicate when curvature effects can be neglected, i.e., when a vertical cylinder can be approximated by a vertical flat plate.

A. Free Convection Case

Figure 1 shows the deviation of the local Nusselt number of a slender cylinder from that of a flat plate for various Prandtl

Table 1 Deviation of local Nusselt number of a heated slender cylinder from that of a heated flat plate for various Prandtl numbers [combined free-forced convection case: $Gr/Re = 1000$, $\beta = 2.07 \times 10^{-4}$ (°C)$^{-1}$]

	$Nu_{x,cyl}/Nu_{x,f.p.}$					
m_x	$Pr =$ 0.1	$Pr =$ 0.72	$Pr =$ 1.0	$Pr =$ 10.0	$Pr =$ 11.4[a]	$Pr =$ 100.0
0.0	1.000	1.000	1.000	1.000	1.000	1.000
0.00036	1.097	1.072	1.068	1.042	1.026	1.024
0.00101	1.129	1.123	1.117	1.074	1.045	1.042
0.00186	1.208	1.166	1.159	1.103	1.062	1.059
0.00286	1.250	1.204	1.195	1.129	1.078	1.075
0.00400	1.288	1.238	1.228	1.153	1.093	1.090
0.00526	1.322	1.268	1.258	1.175	1.108	1.103
0.00663	1.353	1.297	1.285	1.195	1.121	1.117
0.00810	1.382	1.323	1.311	1.215	1.134	1.130
0.00966	1.409	1.347	1.335	1.233	1.146	1.142
0.01131	1.434	1.370	1.357	1.251	1.158	1.153
0.01305	1.458	1.392	1.379	1.268	1.169	1.165
0.01487	1.481	1.413	1.399	1.284	1.180	1.176
0.01677	1.902	1.432	1.418	1.299	1.191	1.186
0.01874	1.523	1.452	1.437	1.314	1.201	1.196
0.02078	1.542	1.470	1.455	1.328	1.211	1.206
0.02290	1.961	1.487	1.472	1.342	1.220	1.216
0.02508	1.580	1.504	1.488	1.355	1.230	1.225
0.02732	1.597	1.520	1.504	1.368	1.239	1.234
0.02963	1.614	1.936	1.519	1.380	1.248	1.243
0.03200	1.631	1.551	1.541	1.392	1.256	1.252

[a]Based on $\Delta\rho = -\rho_0\gamma(\Delta T)^2$ with $\gamma = 8.0 \times 10^{-6}$ (°C)$^{-2}$.

numbers as a function of the transverse curvature parameter that is proportional to $\xi^{1/4}$ for a given Rayleigh number. Here, $\Delta\rho(\Delta T)$ is a linear function, and our results could be directly compared with accepted data points published by Sparrow and Gregg.[1] Computations for water at approximately 4°C, i.e., $0°C < T(\xi,\eta) < 8°C$[5] were carried out with the quadratic relationship for $\Delta\rho(\Delta T)$ and the linear one elsewhere, i.e., when $T(\xi,\eta) \geq 8°C$. We found that transverse curvature effects on the velocity and temperature profiles are significant. As the parameter $\Lambda \sim (x^{1/4}/r_0)$ increases, the boundary layers thicken rapidly. For example, for $\Lambda = 0$, η_∞ is approximately 8.0, and for $\Lambda = 1.0$, η_∞ is about 85. Momentum transfer, which is anyway stronger than thermal diffusion, is further enhanced by the transverse curvature effect. Computer experiments indicated that if

$$[(L/D)/Gr_L^{1/4}] \leq 0.0476$$

curvature effects can be neglected with an error of less than 5%, and a vertical, isothermal cylinder can be treated equivalently as a flat plate.

B. Combined Free-Forced Convection Case

In order to show the deviation of the local Nusselt number for a cylinder from the one for a flat plate, it is most convenient to use the parameter

$$m_x = \frac{L}{D}\frac{Gr_x}{Re_x^{5/2}} \sim \sqrt{x}$$

Table 1 lists values of the ratio of local Nusselt numbers in axial direction for different Prandtl number fluids. For the fluid with $Pr = 11.4$, which corresponds to water at 4°C, the parabolic density function has been employed. The values for the Nusselt number ratio in this column almost coincide with those in the column for $Pr = 100$, which corresponds to an oil with linear density relationship. Computer experiments indicated that if the dimensionless group

$$m_L = \frac{L}{D}\frac{Gr_L}{Re_L^{5/2}} \leq 2.0 \times 10^{-4} \quad \text{for} \quad Pr \geq 0.72$$

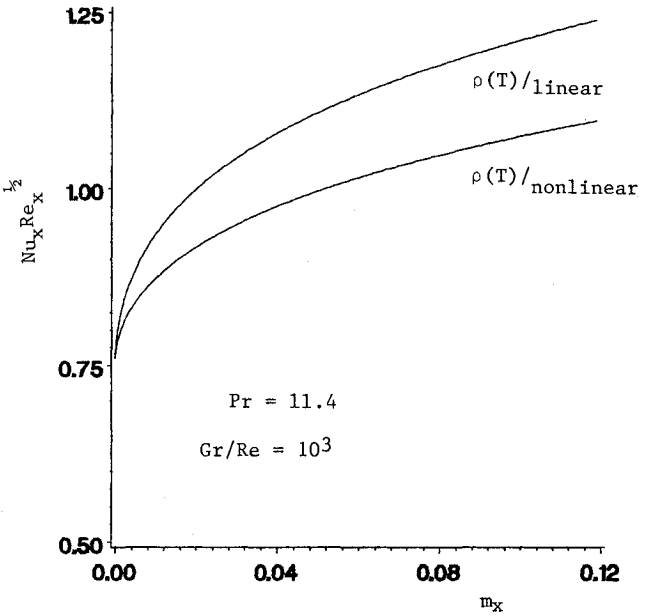

Fig. 2 Distribution of the heat-transfer group along a heated slender cylinder for water with different density representations: mixed convection case.

a heated vertical cylinder can be approximated by a flat plate for Nusselt number computations. This criterion also holds for water at 4°C. The measurable effect of the nonlinear density curve for water is depicted in Fig. 2 in terms of the local heat-transfer group distribution. We also analyzed the effect of transverse curvature on the velocity and temperature profiles for water at about 4°C flowing past heated ($4°C < T_w < 8°C$) and cooled cylinders ($0°C < T_w < 4°C$). In the first case ($Z = 1.0$), free convection heat-transfer mechanisms are supportive in the forced flow development, whereas for $Z = -1.0$, they work against the (forced) upward motion. In order to study the influence of the transverse curvature parameter λ, we consider first a cylinder of constant radius and then of constant length.

For a fixed radius, $\lambda \sim (\sqrt{x}/r_0)$ increases with axial distance and so does the buoyancy force. Larger λ ($\lambda \geq 0.3$) act like favorable pressure gradients and, hence, cause a velocity overshoot when compared with simple forced convection flow past a heated surface. However, for mixed convection flow past a cooled surface, an increase of λ will produce the equivalent of an adverse pressure gradient, i.e., the buoyancy force tends to retard the forced convection flow, and flow separation is possible.

For a fixed distance, an increase of λ corresponds to a more slender cylinder that changes predominantly the velocity profiles of flow past a heated cylinder, significantly.

References

[1]Sparrow, E. M. and Gregg, J. L., "Laminar Free Convection Heat Transfer from the Outer Surface of a Vertical Circular Cylinder," *Transactions of the ASME*, Vol. 78, American Society of Mechanical Engineers, 1956, pp. 1823-1829.

[2]Wilks, G., "Combined Forced and Free Convection Flow on a Vertical Surface," *International Journal of Heat and Mass Transfer*, Vol. 16, 1973, pp. 1958-1963.

[3]Minkowycz, W. J. and Sparrow, E. M., "Local Nonsimilar Solutions for Natural Convection on a Vertical Cylinder," *Journal of Heat Transfer*, Vol. 96, May 1974, pp. 178-183.

[4]Bui, M. N. and Cebeci, T., "Combined Free and Forced Convection on Vertical Slender Cylinders," *Journal of Heat Transfer*, Vol. 107, May 1985, pp. 476-478.

[5]Goren, S. L., "On Free Convection in Water at 4°C," *Chemical Engineering Science*, Vol. 21, 1966, pp. 515-518.

[6]Soundalgekar, V. H., Ramana Murty, T. W., and Vighnesam, N. V., "Combined Forced and Free Convection Flow of Water at 4°C Past a Semi-Infinite Vertical Plate," *International Journal of Heat and Fluid Flow*, Vol. 5, March 1984, pp. 54-56.

[7]Gorla, R. S. R. and Stratman, R. A., "Natural Convection Boundary Layer Flow of Water at 4°C Past Slender Cones," *International Communications in Heat and Mass Transfer,* Vol. 13, 1986, pp. 403–411.

[8]Kleinstreuer, C. and Eghlima, A., "Analysis and Simulation of New Approximation Equations for Boundary-Layer Flow on Curved Surfaces," *Mathematics and Computers in Simulations,* Vol. 27, 1985, pp. 307–325.

[9]Kleinstreuer, C., *Engineering Fluid Dynamics—An Interdisciplinary Systems Approach,* Springer-Verlag, New York, 1989 (to be published).

[10]Cebeci, T. and Bradshaw, P., *Momentum Transfer in Boundary Layers,* Hemisphere Pub., Washington, DC, 1977.

Implicit Flux-Split Algorithm to Calculate Hypersonic Flowfields in Chemical Equilibrium

Grant Palmer*
NASA Ames Research Center,
Moffett Field, California

Introduction

THE aeroassisted orbital transfer vehicle (AOTV) and the national aerospace plane will be required to maneuver at hypersonic velocities in the upper atmosphere in flow regimes where the ideal gas assumption does not apply. The design of these vehicles will depend on a new generation of numerical algorithms that combine the gasdynamic equations of computational fluid dynamics with equilibrium and nonequilibrium chemical reactions. The first step in developing a hypersonic computational fluid dynamics capability is a solid equilibrium code, one that is efficient and stable.

In recent years, a number of attempts have been made to simulate real-gas flowfields about blunt bodies.[1-3] This study presents an implicit, shock-capturing algorithm for calculating hypersonic equilibrium flow over blunt bodies. The fluxes are diferenced using first-order Steger-Warming[4] flux vector splitting. The equilibrium chemistry package is based on the Gibbs free energy minimization technique of Gordon and McBride.[5]

The present algorithm has shown itself to be robust and efficient. The techniques used are easy to understand and allow the code to be written in a modular, straightforward manner. Modifications and extensions are easily implemented. The code has proved its ability to capture strong shocks about blunt bodies at hypersonic velocities.

Governing Equations

The Euler equations for two-dimensional or axisymmetric perfect gas flow without external forces can be expressed in conservation law form in generalized coordinates[6] as

$$\frac{\partial Q}{\partial t}+\frac{\partial F}{\partial \xi}+\frac{\partial G}{\partial \eta}+rH=0 \tag{1}$$

with

$$Q=J^{-1}\begin{bmatrix}\rho\\ \rho u\\ \rho v\\ e\end{bmatrix} \qquad F=J^{-1}\begin{bmatrix}\rho U\\ \rho uU+\xi_x p\\ \rho vU+\xi_y p\\ (e+p)U\end{bmatrix}$$

$$G=J^{-1}\begin{bmatrix}\rho V\\ \rho uV+\eta_x p\\ \rho vV+\eta_y p\\ (e+p)V\end{bmatrix} \qquad H=\frac{J^{-1}}{y}\begin{bmatrix}\rho v\\ \rho uv\\ \rho v^2\\ (e+p)v\end{bmatrix}$$

It is necessary to relate the pressure to the flow variables. The parameter β is introduced and defined as the ratio of static enthalpy to internal energy. For an ideal gas, β equals the ratio of specific heats, γ. Expressing the internal energy in terms of the flow variables and the static enthalpy in terms of β, p, and ρ yields the desired equation of state:

$$p=(\beta-1)[e-\tfrac{1}{2}\rho(u^2+v^2)] \tag{2}$$

Method

The basic form of the algorithm is the Beam and Warming approximate factorization algorithm[7]

$$(I+\Delta t\delta_\xi A^n)[I+\Delta t(\delta_\eta B^n+rC^n)]\delta Q^n$$
$$=-\Delta t(\delta_\xi F^n+\delta_\eta G^n+rH^n) \tag{3}$$

The spatial derivatives are differenced using an upwind technique: that of Steger-Warming flux vector splitting.[4] The first-order flux-split technique is naturally stable and easy to code. Strong shocks can be captured without artificial dissipation terms or flux limiters. For viscous flows, first-order differencing is too dissipative to resolve the boundary layer accurately, but for inviscid flow calculations this dissipative nature is not as big a concern. Proper selection of the grid and the use of solution grid adaption techniques minimize any inaccuracies and shock smearing caused by the first-order method. Accurate results were obtained for a Mach 20 hemisphere test problem using the first-order method.

Steger-Warming flux vector splitting is based on the fact that the Euler equations are homogenous of degree one, such that $F=AQ$ and $G=BQ$. The flux vector F is split into positive and negative components:

$$F=F^+ +F^- =A^+Q+A^-Q \tag{4}$$

$$A^+=S_A\Lambda_A^+S_A^{-1} \qquad A^-=S_A\Lambda_A^-S_A^{-1} \tag{5}$$

The matrices Λ_A^+ and Λ_A^- contain the positive and negative eigenvalues of A, respectively, and S_A is the eigenvector matrix of A. The matrices G and B are similarly split. From domain of dependence and linear stability considerations, backward-difference approximations are used for the positive fluxes and positive-flux Jacobians and forward-difference approximations are used for the negative fluxes and negative-flux Jacobians.

Boundary Conditions

Along the body surface, the tangent Cartesian velocity components are found by setting V equal to zero and extrapolating U from the interior.[6] The freestream total enthalpy, $(e+p)/\rho$, is assumed constant along the body. This assumption is acceptable for steady-state calculations.

One additional parameter, for instance pressure, is necessary to determine the flow quantities along the wall boundary. The normal momentum equation can be used to determine this pressure. It is generally written in nonconservative form.[6] It was desired to use an impulsive starting procedure with the

Presented as Paper 87-1580 at the AIAA 22nd Thermophysics Conference, Honolulu, HI, June 8–10, 1987; received June 25, 1987; revision received Oct. 19, 1987.

*Research Scientist. Member AIAA.